

Schwinger instability, modular flow, and holographic entropy for near-extremal charged BTZ black hole

Mendrit Latifi* and Kimet Jusufi†

*Institute for Theoretical Physics, Heidelberg University,
Philosophenweg. 19, 69117 Heidelberg, Germany and*

*Physics Department, University of Tetova, Ilinden Street nn, 1200, Tetovo, North Macedonia
(Dated: May 26, 2025)*

We investigate the quantum dynamics of a charged scalar field in the near-horizon region of a near-extremal charged BTZ black hole. A controlled expansion of the Einstein–Maxwell equations reveals an emergent warped $\text{AdS}_2 \times S^1$ throat geometry threaded by a constant electric field—an ideal setting for studying Schwinger pair production, Hawking radiation, and entropy flow. By solving the Klein–Gordon equation using both tunneling and field-theoretic methods, we compute the pair production rate and identify an effective Unruh-like temperature. In particular, we apply the WKB approximation for Hawking tunneling, justified by the infinite blueshift experienced by outgoing modes near the horizon. Instability arises when local acceleration exceeds the AdS curvature scale, linking near-horizon dynamics to thermal emission. Through the generalized uncertainty principle, which leads to the existence of the minimal length, we argue that quantum gravity effects can lead to a vanishing Hawking and Schwinger-like temperature. To connect quantum radiation to geometry, we analyze the flux of the modular Hamiltonian across the horizon and show that its variation precisely matches the entropic contribution of the produced pairs. Using Tomita–Takesaki theory and the Type II_∞ von Neumann algebra of horizon observables, we derive a semiclassical gravitational constraint involving the second variation of the stress tensor—recovering the null-null Einstein equation from entropy extremization. The intersection point of inward and outward RT geodesics marks both the peak of pair production and the vanishing of entropy variation, revealing a deep geometric alignment between entanglement, quantum matter, and backreaction. The near-horizon geometry does not merely support quantum effects—it organizes them.

I. INTRODUCTION

Black holes are more than gravitational solutions to Einstein’s equations—they are profound windows into the quantum nature of spacetime. Ever since Hawking’s discovery that black holes radiate [1–3] and Bekenstein’s insight that they carry entropy proportional to their horizon area [4], these objects have stood at the frontier of our efforts to unify general relativity and quantum mechanics. The thermodynamic behavior of black holes [5–7] has reshaped our understanding of entropy, information, and the very fabric of spacetime.

Lower-dimensional models, such as the charged BTZ black hole in $(2 + 1)$ dimensions [8–10], offer a uniquely tractable framework for exploring these ideas. These spacetimes are simple enough to allow exact calculations, yet rich enough to capture essential features of black hole thermodynamics, causal structure, and holography [11]. In particular, the near-extremal limit of charged black holes reveals a long AdS_2 throat—a geometric hallmark that underlies much of the recent progress in AdS/CFT [12–14] and related approaches to low-dimensional gravity.

This AdS_2 structure also plays a central role in the study of quantum chaos [15], nearly conformal quantum mechanics [16], and entanglement dynamics in gravitational

systems [17, 18]. From the perspective of the dual theory, it supports a well-defined notion of modular flow, thermal states, and vacuum correlations that extend naturally to holographic entanglement calculations.

Beyond their geometric simplicity, near-extremal black holes offer a well-controlled arena for semiclassical computations. Quantum corrections to black hole entropy in these backgrounds can be calculated using the quantum entropy function (QEF) formalism [19–21], which systematically includes one-loop effects from quantum fields propagating in the AdS_2 throat. These corrections, often captured via heat kernel or zeta-function methods [22–25], reveal universal logarithmic terms and entanglement contributions consistent with expectations from holography [26–28].

In this work, we explore how the Schwinger effect—the spontaneous creation of charged pairs in strong electric fields [29–34]—arises in the near-horizon region of a near-extremal charged BTZ black hole. Using a controlled expansion in the deviation from extremality, we construct an analytically tractable background geometry and solve the Klein–Gordon equation for a charged scalar field. The resulting pair production rate encodes a vacuum instability localized near the bifurcation surface and reflects the onset of quantum backreaction.

We complement this analysis with a semiclassical treatment of Hawking radiation, interpreting it as a tunneling process of charged particles across the horizon. By evaluating the imaginary part of the classical action in the WKB approximation, we derive the Hawking temperature directly from the tunneling amplitude. This frame-

* ljatifi@thphys.uni-heidelberg.de

† kimet.jusufi@unite.edu.mk

work allows us to define both a thermal and electric contribution to the emission spectrum and to compare the onset of instability with the effective Unruh temperature associated with acceleration in the near-horizon region.

Crucially, we go further and ask how this quantum radiation feeds back into the spacetime itself. Working in a semiclassical regime, we analyze how the stress-energy tensor of the quantum field perturbs the background geometry. We show that the modular Hamiltonian flux across the past horizon, derived from operator-algebraic methods, captures the leading-order backreaction from pair production. Demanding that the generalized entropy remain stationary leads to a gravitational constraint that matches the null-null component of the semiclassical Einstein equations. This aligns with Jacobson's perspective that gravity emerges from thermodynamics and entropy flow [35], now extended to include quantum fields and modular energy.

To formalize this connection, we adopt the operator-algebraic language of Tomita–Takesaki theory [36–39], where observables on the horizon form a semifinite von Neumann algebra. The modular Hamiltonian associated with the Hartle–Hawking vacuum generates a nontrivial flow whose flux across the horizon quantifies entanglement and backreaction in a unified manner.

Our central finding is that geometry, quantum matter, and operator algebras converge in a highly structured way. The region where Schwinger pair production is most active coincides with the point where inward and outward Ryu–Takayanagi [40–42] (RT) surfaces intersect and where the variation of generalized entropy vanishes. This striking coincidence reveals that the geometry does not simply accommodate quantum effects—it shapes and organizes them through a delicate interplay of curvature, entanglement, and modular flow.

The paper is organized as follows. In Sec. II, we obtain a near-horizon geometry of the near-extreme charged BTZ black hole. In Sec. III, we study the Schwinger effect. In Sec. IV, and V we study Hawking radiation via quantum tunneling and the quantum gravity effects. In Sec. VI and Sec. VII, we elaborate more on the quantum entropy and modular flow. In Sec. VIII, we comment on our findings.

II. NEAR-HORIZON GEOMETRY OF THE NEAR-EXTREMAL CHARGED BTZ BLACK HOLE

We begin with the Einstein–Maxwell system in $(2+1)$ dimensions with a negative cosmological constant, which serves as the effective description of charged black holes in asymptotically AdS_3 spacetimes [8–10]. The action is given by:

$$S = \int d^3x \sqrt{-g} \left(R - 2\Lambda - \frac{1}{4} F_{\mu\nu} F^{\mu\nu} \right), \quad (1)$$

where $\Lambda = -1/\ell^2$ is the AdS curvature scale. Varying this action yields the Einstein and Maxwell field equations:

$$R_{\mu\nu} - \frac{1}{2} g_{\mu\nu} R + \Lambda g_{\mu\nu} = 8\pi G T_{\mu\nu}, \quad (2)$$

$$\nabla_\mu F^{\mu\nu} = 0. \quad (3)$$

The general solution corresponding to a charged BTZ black hole takes the form [9]:

$$ds^2 = -f(r) dt^2 + \frac{dr^2}{f(r)} + r^2 d\phi^2, \quad (4)$$

with lapse function:

$$f(r) = -M + \frac{r^2}{\ell^2} - \frac{Q^2}{2} \ln \left(\frac{r}{r_0} \right), \quad (5)$$

and gauge potential:

$$A_\mu = \left(-Q \ln \left(\frac{r}{r_0} \right), 0, 0 \right), \quad (6)$$

where M and Q are the ADM mass and charge, respectively, and r_0 is a reference scale associated with the boundary subtraction scheme [10].

The extremal limit corresponds to the case where the black hole temperature vanishes. This occurs when the inner and outer horizons coincide, i.e., when the lapse function and its derivative vanish at the extremal radius $r = r_e$:

$$f(r_e) = 0, \quad f'(r_e) = 0. \quad (7)$$

Solving these conditions gives:

$$M_{\text{ext}} = \frac{r_e^2}{\ell^2} - \frac{Q_{\text{ext}}^2}{2} \ln \left(\frac{r_e}{\ell} \right), \quad (8)$$

$$Q_{\text{ext}}^2 = \frac{4r_e^2}{\ell^2}. \quad (9)$$

This extremal solution plays a central role in AdS_2 holography and appears universally in near-extremal limits of many higher-dimensional black holes [11, 13].

To study departures from extremality, we introduce a small parameter $\epsilon \ll 1$ and expand around the extremal point. The charge and coordinate system are modified as:

$$Q^2 = Q_{\text{ext}}^2 (1 - \epsilon), \quad (10)$$

$$r = r_e + \epsilon \rho, \quad t = \frac{T}{\epsilon}. \quad (11)$$

This change of coordinates captures the near-horizon, near-extremal region where quantum effects such as the Schwinger mechanism become significant [31, 33, 34].

Expanding the lapse function (5) to leading order in ϵ yields:

$$f(r) \approx \frac{(2 - \epsilon)}{\ell^2} \epsilon^2 \rho^2 + \mathcal{O}(\epsilon^3), \quad (12)$$

which implies the near-horizon metric takes the form:

$$ds^2 = -\frac{(2-\epsilon)}{\ell^2}\rho^2 dT^2 + \frac{\ell^2}{(2-\epsilon)\rho^2}d\rho^2 + r_e^2 d\phi^2. \quad (13)$$

To the best of our knowledge, this specific form of the near-extremal, near-horizon charged BTZ metric with controlled ϵ -dependence has not appeared explicitly in the literature. This is a warped product of AdS_2 and a fixed-radius circle S^1 , with ϵ -dependent correction to the AdS curvature scale. One can easily check the Ricci tensor components

$$R_{\rho\rho} = -\frac{1}{\rho^2}, \quad R_{TT} = \frac{(2-\epsilon)^2\rho^2}{\ell^4}, \quad (14)$$

and the Riemann tensor components

$$R_{\rho T \rho T} = -\frac{1}{\rho^2}, \quad R_{\rho T T \rho} = -\frac{(2-\epsilon)^2\rho^2}{\ell^4}. \quad (15)$$

Let us also mention that the spacetime is free from physical singularities; it has a finite and regular Ricci scalar and Kretschmann scalar

$$R = -\frac{6}{\ell^2}, \quad K = \frac{36}{\ell^4}. \quad (16)$$

However, this spacetime has a coordinate singularity at $\rho = 0$. One way to see this is to study the “coordinate speed of light” by setting $ds^2 = d\phi^2 = 0$, we get

$$\left. \frac{d\rho}{dT} \right|_{\rho=0} = \pm \frac{2-\epsilon}{\ell^2} \rho^2 \Big|_{\rho=0} \longrightarrow 0, \quad (17)$$

which shows the presence of coordinate singularity. The geometry (13) exhibits three essential features:

1. An emergent AdS_2 throat parametrized by (ρ, T) , with effective curvature radius $\ell/\sqrt{2-\epsilon}$, typical of near-horizon limits of extremal black holes [43, 44].
2. A compact angular dimension ϕ with radius r_e , which remains fixed as $\epsilon \rightarrow 0$ and sets the transverse size of the throat [8].
3. A gauge potential that simplifies in this limit. Using the expansion:

$$A_T \approx -Q \left[\ln \left(\frac{r_e}{r_0} + \frac{\epsilon\rho}{r_e} \right) \right] + \mathcal{O}(\epsilon^2) \quad (18)$$

we see that the near-horizon electric field becomes approximately constant. This supports a Schwinger effect in the AdS_2 background, much like in higher-dimensional charged black holes [32, 45, 46].

This near-horizon limit provides a robust and analytically controlled setting to study quantum field theory in curved spacetime. In the sections that follow, we use this geometry to examine both the instability induced by charged pair production and the modular structure of the resulting quantum state.

III. SCHWINGER PAIR PRODUCTION IN NEAR-EXTREMAL BTZ BLACK HOLES

Quantum fluctuations in curved spacetime can spontaneously produce particle-antiparticle pairs unless suppressed by the geometry or background fields. In black hole spacetimes, the event horizon acts as a causal barrier that separates such pairs, enabling the black hole to radiate all species of particles. This mechanism becomes particularly interesting for charged black holes.

Extremal charged black holes, despite having zero Hawking temperature, can still support quantum emission through the Schwinger effect—a nonthermal tunneling process driven by the background electric field [1, 29]. In the near-extremal regime, the geometry near the horizon develops an emergent $\text{AdS}_2 \times S^1$ throat. This structure allows for a precise analytic treatment of pair creation using methods developed in [31, 33, 34].

We consider a minimally coupled, charged scalar field Φ with mass m and charge q . Its action is:

$$S = \int d^3x \sqrt{-g} \left(-\frac{1}{2} D_\mu \Phi^* D^\mu \Phi - \frac{1}{2} m^2 \Phi^* \Phi \right), \quad (19)$$

where $D_\mu = \nabla_\mu - iqA_\mu$ is the gauge-covariant derivative. The field satisfies the Klein-Gordon equation:

$$(\nabla_\mu - iqA_\mu)(\nabla^\mu - iqA^\mu)\phi - m^2\phi = 0. \quad (20)$$

We solve this equation using separation of variables:

$$\Phi(T, \rho, \phi) = e^{-i\omega T} H_L(\phi) R(\rho), \quad (21)$$

where $H_L(\phi)$ is the eigenfunction of the angular Laplacian on S^1 , satisfying $\nabla_\perp^2 H_L = -L^2 H_L$.

The radial equation in the near-horizon, near-extremal metric (cf. Section II) becomes:

$$\begin{aligned} \rho^2 R''(\rho) + 2\rho R'(\rho) + \frac{\ell^4 \omega_0^2}{(2-\epsilon)^2} \cdot \frac{1}{\rho^2} R(\rho) \\ - \frac{2\ell^4 \omega_0 q Q \epsilon}{r_e (2-\epsilon)^2} \cdot \frac{1}{\rho} R(\rho) \\ - \frac{\ell^2 (m^2 + \frac{L^2}{r_e^2})}{(2-\epsilon)} R(\rho) = 0. \end{aligned} \quad (22)$$

Defining constants A, B and C_0 as

$$A = \frac{\ell^4 \omega_0^2}{(2-\epsilon)^2}, \quad (23)$$

$$B = \frac{2\ell^4 \omega_0 q Q \epsilon}{r_e (2-\epsilon)^2}, \quad (24)$$

$$C_0 = \frac{\ell^2 (m^2 + \frac{L^2}{r_e^2})}{(2-\epsilon)}. \quad (25)$$

where ω_0 is given by:

$$\omega_0 = \omega - qQ \ln \left(\frac{r_e}{r_0} \right). \quad (26)$$

For the radial equation we can write

$$\rho^2 R''(\rho) + 2\rho R'(\rho) + \left(\frac{A}{\rho^2} - \frac{B}{\rho} - C_0 \right) R(\rho) = 0. \quad (27)$$

We use a coordinate transformation

$$z = \frac{ik}{\rho} \quad \text{where} \quad k = \frac{2\ell^2 \omega_0}{(2 - \epsilon)}, \quad (28)$$

to get the following equation

$$R''(z) + \left[-\frac{A}{k^2} + \frac{iB}{kz} - \frac{C_0}{z^2} \right] R(z) = 0, \quad (29)$$

which can be matched to the standard Whittaker form:

$$\partial_z^2 R(z) + \left[-\frac{1}{4} + \frac{ia}{z} + \frac{1/4 - b^2}{z^2} \right] R(z) = 0. \quad (30)$$

where a and b now are given by:

$$a = \frac{\ell^2 q Q \epsilon}{r_e (2 - \epsilon)} \\ b = \sqrt{\frac{\ell^2 (m^2 + \frac{L^2}{r_e^2})}{(2 - \epsilon)} + \frac{1}{4}}. \quad (31)$$

which can be found from:

$$\frac{A}{k^2} = \frac{1}{4}, \\ \frac{B}{k} = a, \\ C_0 = b^2 - \frac{1}{4}. \quad (32)$$

Equation (30) has solutions in terms of Whittaker functions

$$M_{\kappa, \mu}(z) = e^{-z/2} z^{1/2\mu} F(1/2 + \mu + \kappa, 1 + 2\mu, z) \\ W_{\kappa, \mu}(z) = e^{-z/2} z^{1/2\mu} U(1/2 + \mu + \kappa, 1 + 2\mu, z). \quad (33)$$

which can be related to other special functions, such as hypergeometric functions [31]:

$$W_{\kappa, \mu}(z) = z^{\mu + \frac{1}{2}} e^{-z/2} U\left(\mu - \kappa + \frac{1}{2}, 2\mu + 1, z\right) \quad (34)$$

and $M_{\kappa, \mu}(z)$:

$$M_{\kappa, \mu}(z) = z^{\mu + \frac{1}{2}} e^{-z/2} M\left(\mu - \kappa + \frac{1}{2}, 2\mu + 1, z\right). \quad (35)$$

where $M(a, b, z)$ is given in term of Kummer confluent hypergeometric function as:

$$M(a, b, z) = {}_1F_1(a, b, z) = \sum_{n=0}^{\infty} \frac{(a)_n}{(b)_n} \frac{z^n}{n!}, \quad (36)$$

and $(a)_n$ is the Pochhammer symbol where $(a)_n = a(a+1)(a+2)\dots(a+n-1)$. This function is usually regular at $z = 0$ and does not decay as $z \rightarrow \infty$ (it usually grows).

The general solution to the radial equation (30) is then:

$$R(\rho) = C_1 M_{ia, -b}(z) + C_2 M_{ia, b}(z). \quad (37)$$

where $\kappa = ia$ and $\mu = b$. From the radial solutions we can find the instability (stability) regions:

• Instability region

An instability will occur when

$$\frac{\ell^2 (m^2 + \frac{L^2}{r_e^2})}{(2 - \epsilon)} + \frac{1}{4} < 0, \quad (38)$$

Let us define an effective mass parameter:

$$m_{\text{eff}}^2 = m^2 + \frac{L^2}{r_e^2} \quad (39)$$

where

$$R_{\text{AdS}}^2 = \frac{\ell^2}{(2 - \epsilon)}. \quad (40)$$

Then in term of the effective mass we have

$$\tilde{m}_{\text{eff}}^2 < -\frac{1}{R_{\text{AdS}}^2}, \quad (41)$$

where $\tilde{m}_{\text{eff}}^2 = 4m_{\text{eff}}^2$. It can be easily shown that the instability condition can be expressed also in terms of charge Q as follows

$$\tilde{m}_{\text{eff}}^2 < -\frac{Q_{\text{ext}}^2 + Q^2}{\ell^2 Q_{\text{ext}}^2}, \quad (42)$$

from where it follows that

$$R_{\text{AdS}}^2 = \left(1 + \frac{Q^2}{Q_{\text{ext}}^2}\right) \ell. \quad (43)$$

This shows that with the increase of charge Q the R_{AdS} increases.

• Stability region

For the stability region will we will have

$$\frac{\ell^2 (m^2 + \frac{L^2}{r_e^2})}{(2 - \epsilon)} + \frac{1}{4} \geq 0, \quad (44)$$

which in term of the effective mass, reads

$$\tilde{m}_{\text{eff}}^2 \geq -\frac{1}{R_{\text{AdS}}^2}. \quad (45)$$

The last relation is known as the Breitenlohner-Freedman (BF) bound (see, for example, [31]). In a similar way we express the stability condition in terms of charge Q as follows

$$\tilde{m}_{\text{eff}}^2 \geq -\frac{Q_{\text{ext}}^2 + Q^2}{\ell^2 Q_{\text{ext}}^2}. \quad (46)$$

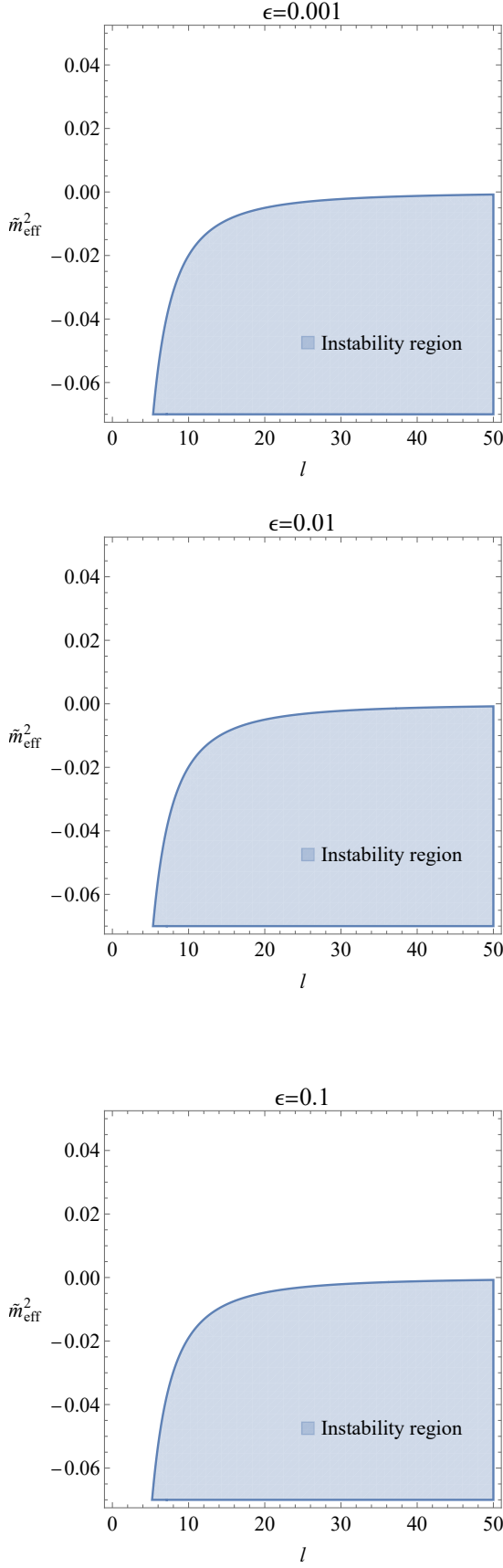


FIG. 1: The instability (stability) region for different values of ϵ , respectively.

Violation of this bound indicates the onset of a tachyonic instability and signals the activation of the Schwinger effect in the presence of a strong electric field.

In Fig. 1, we plot the instability region in the $(\ell, \tilde{m}_{\text{eff}}^2)$ -plane for various values of the deviation parameter ϵ . The shaded region indicates where the Breitenlohner–Freedman (BF) bound is violated, signaling the onset of tachyonic instability due to Schwinger pair production. As ℓ increases, the instability region expands rapidly and saturates, reflecting the fact that the effective AdS₂ curvature scale grows with ℓ . For small values of ϵ , corresponding to nearly extremal black holes, the instability region is wider—consistent with the idea that the near-horizon AdS₂ throat becomes longer and supports more IR-sensitive modes. This demonstrates that the system is most unstable near extremality and that the instability becomes more pronounced in the large ℓ regime.

In Figure 2, we show how the instability region varies with the black hole charge Q for fixed values of AdS radius ℓ . For each case, the shaded area corresponds to values of \tilde{m}_{eff}^2 that lie below the BF bound. As Q approaches its extremal value, the instability region shrinks—indicating that the system becomes more stable near extremality. This is consistent with the known suppression of the Schwinger effect in extremal geometries, where the Hawking temperature vanishes and the near-horizon electric field becomes too weak to support pair production. The higher the value of ℓ , the larger the instability region, but in all cases, extremality ($Q \rightarrow Q_{\text{ext}}$) marks the boundary of stability. This provides clear numerical evidence that extremal black holes are more stable against charged scalar instabilities, consistent with the findings of [33].

The flux associated with the scalar field is [31]:

$$D = i\sqrt{-g}g^{\rho\rho}(\Phi D_\rho \Phi^* - \Phi^* D_\rho \Phi). \quad (47)$$

To model spontaneous pair creation in the near-horizon region, we solve the radial wave equation and analyze the behavior of its solutions near the outer boundary ($z \rightarrow 0$) and near the horizon ($z \rightarrow \infty$). The radial solution given by (37) with parameters given by (31) and ω_0^2 given by (26). The general solution (37) exhibit the following asymptotic behaviors: near the boundary ($z \rightarrow 0$),

$$M_{ia,\pm b}(z) \sim z^{1/2 \pm b} e^{z/2}, \quad (48)$$

and near the horizon ($z \rightarrow \infty$),

$$M_{ia,\pm b}(z) \sim e^{-z/2} z^{1/2 \pm ia}. \quad (49)$$

At the boundary $z \rightarrow 0$, the solution behaves as

$$R_B(z) \sim c_B^{(\text{in})} z^{1/2+ib} + c_B^{(\text{out})} z^{1/2-ib}, \quad (50)$$

which identifies the coefficients $c_B^{(\text{in})} = c_1$ and $c_B^{(\text{out})} = c_2$ as incoming and outgoing wave amplitudes, respectively. To model spontaneous pair production, we impose the

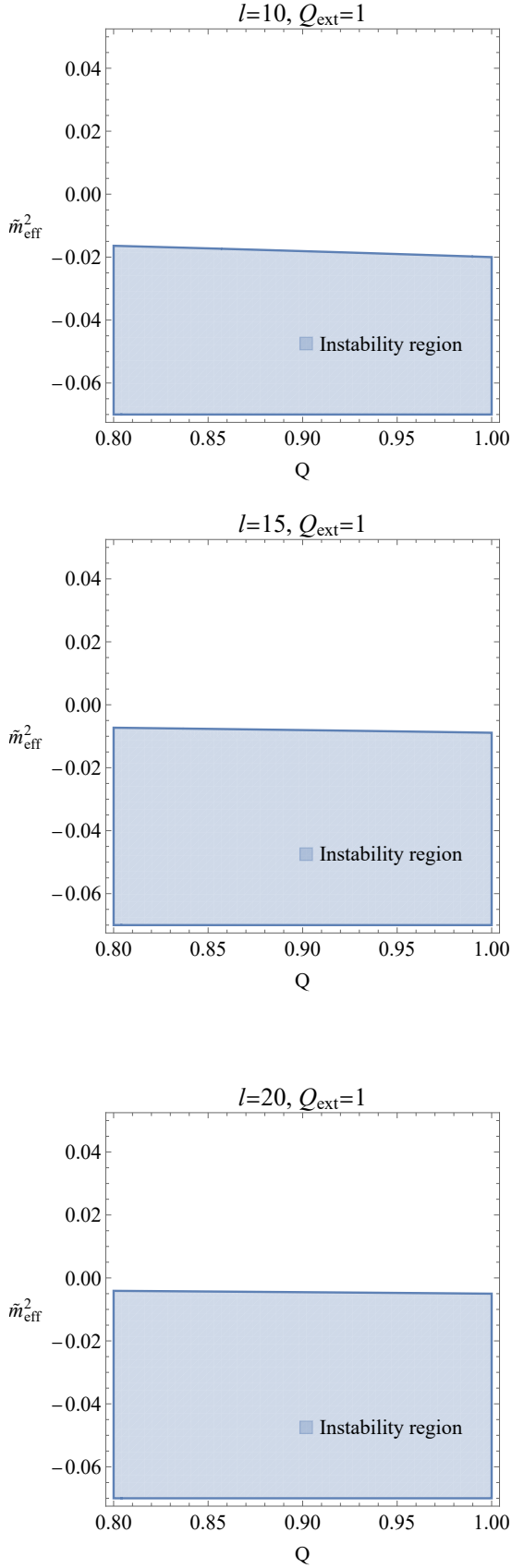


FIG. 2: The instability (stability) region for fixed values of l , and varying charge.

physically motivated boundary condition that no flux comes in from infinity, i.e., $D_B^{(\text{in})} = 0$, which sets $c_1 = 0$. At the horizon, both ingoing and outgoing modes are allowed, and the flux can be computed using (47). Substituting the Whittaker solution and using analytic continuation of hypergeometric functions, one finds that the outgoing flux at the boundary is

$$D_B^{(\text{out})} = 2\omega Q^2 (2b e^{\pi b}) |c_2|^2, \quad (51)$$

while the incoming and outgoing fluxes at the horizon are

$$D_H^{(\text{in})} = -2\omega Q^2 e^{\pi a} |c_H^{(\text{in})}|^2, \quad (52)$$

$$D_H^{(\text{out})} = +2\omega Q^2 e^{-\pi a - 2\pi b} |c_B^{(\text{out})}|^2. \quad (53)$$

The Bogoliubov coefficient β quantifies the mean number of pairs produced and is obtained from the ratio of outgoing flux at the boundary to the incoming flux at the horizon. Using the results from [31, 32, 34, 47], one finds

$$|\beta|^2 = \frac{D_B^{(\text{out})}}{D_H^{(\text{in})}} = \frac{\sinh(2\pi b)}{\cosh(\pi a + \pi b)} e^{\pi b - \pi a}. \quad (54)$$

This is the exact expression for the mean number of produced pairs:

$$\mathcal{N} = \frac{\sinh(2\pi b)}{\cosh(\pi a + \pi b)} e^{\pi b - \pi a}. \quad (55)$$

Unlike Hawking radiation, which is thermal and governed by the black hole's surface gravity, the Schwinger process is a non-thermal, purely quantum phenomenon. It originates from vacuum polarization in strong electric fields, as in flat-space QED [32, 45, 46], but is dramatically enhanced in the near-horizon AdS_2 geometry due to the spacetime curvature and redshift.

1. Semiclassical Schwinger tunneling rate

We will show that the expression for the mean number of produced pairs reduces to the semiclassical Schwinger tunneling rate in the appropriate limit. To see this, we need to consider the regime where $a \gg b$ is satisfied, i.e., corresponding to a sufficiently strong electric field. In this limit Eq. (55) becomes

$$\mathcal{N} \sim e^{-\pi a}. \quad (56)$$

To relate this to physical quantities, we recall that $b = m_{\text{eff}}^2 R_{\text{AdS}}$, where $m_{\text{eff}}^2 = m^2 + \frac{L^2}{r_e^2}$ is the effective mass squared and $R_{\text{AdS}}^2 = \frac{\ell^2}{2-\epsilon}$ is the curvature radius squared of the near-horizon AdS_2 region. The parameter a depends on the electric field and redshifted energy, where we can compute the electric field in new coordinates

$$\mathcal{E} = -\frac{\partial A_T}{\partial \rho} = \epsilon Q / r_c + \mathcal{O}(\epsilon \rho) \quad (57)$$

Using the above equations for a in (31) we can write

$$a = \frac{q\mathcal{E}\ell^2}{2-\epsilon}. \quad (58)$$

If we now use the following condition (which will be explained in more details next section)

$$\frac{\ell^2}{2-\epsilon} = \left(\frac{m_{\text{eff}}}{q\mathcal{E}}\right)^2, \quad (59)$$

we get

$$a = \frac{m_{\text{eff}}^2}{q\mathcal{E}}. \quad (60)$$

Substituting into the exponent yields

$$\mathcal{N} \sim \exp\left(-\frac{\pi m_{\text{eff}}^2}{q\mathcal{E}}\right), \quad (61)$$

which is the expression for the semiclassical Schwinger tunneling rate.

IV. QUANTUM TUNNELING OF CHARGED SCALAR PARTICLES

Let us elaborate and consider in more detail the Hawking radiation in terms of the tunneling approach for the case of charged scalar particle in the spacetime (13). The Klein-Gordon equation reads

$$\frac{1}{\sqrt{-g}}(\partial_\mu - \frac{iq}{\hbar}A_\mu)\left(\sqrt{-g}g^{\mu\nu}(\partial_\mu - \frac{iq}{\hbar}A_\mu)\Phi\right) - \frac{m^2}{\hbar^2}\Phi = 0, \quad (62)$$

where m and q are the mass and charge of the particle, respectively. We will make use of the WKB ansatz,

$$\Phi = \exp\left(\frac{i}{\hbar}S(t, u, \phi)\right), \quad (63)$$

where we will work in terms of time coordinate t which is related to T via $T = \epsilon t$. In general, one can assume the form of action $S(t, \rho, \phi)$ in a powers of \hbar as follows

$$S(t, \rho, \phi) = S_0(t, \rho, \phi) + \sum_{i=1} \hbar^i S_i(t, \rho, \phi). \quad (64)$$

Taking into the consideration the symmetries of the metric by corresponding Killing vectors $(\partial/\partial t)^\mu$ and $(\partial/\partial \phi)^\mu$, the action as the following form

$$S_0(t, \rho, \phi) = -Et + R(\rho) + L\phi, \quad (65)$$

where E is the energy of the particle, and L denotes the angular momentum of the particle corresponding to the angles ϕ . As noted in [7], the WKB approximation can be justified due to the following argument: It is expected that the typical wavelength of the radiation to be of the

order of the size of the horizon, however, when the outgoing wave is traced back towards the horizon, its wavelength as measured by an static observers is increasingly blue-shifted. Near the horizon, the radial wavenumber approaches infinity and the point particle, or WKB, approximation is justified. From the above equations in the leading order terms in \hbar , we obtain the following equation

$$\begin{aligned} & -\frac{(2-\epsilon)\rho^2}{\ell^2}\left(\frac{d}{d\rho}R(\rho)\right)^2 + \frac{\ell^2(E + qA_t)^2}{(2-\epsilon)\rho^2\epsilon^2} \\ & - \left(m^2 + \frac{L^2}{r_e^2}\right) = 0 \end{aligned} \quad (66)$$

from where we get the radial part $R(u)$ as follows

$$R_\pm = \pm \int \frac{\ell^2}{(2-\epsilon)} \frac{\sqrt{(E + qA_t)^2 - \rho^2\epsilon^2 \frac{(2-\epsilon)m_{\text{eff}}^2}{\ell^2}}}{\rho^2\epsilon} d\rho \quad (67)$$

To evaluate this integral, we first define the function $\mathcal{F}(\rho) = \rho^2\epsilon(2-\epsilon)/\ell^2$, and we consider a series expansions around ρ_+ , namely

$$\mathcal{F}(\rho) \simeq \rho_+^2\epsilon(2-\epsilon)/\ell^2 + \mathcal{F}'(\rho)|_{\rho=\rho_+}(\rho - \rho_+) \quad (68)$$

where $\mathcal{F}'(\rho)|_{\rho=\rho_+} \simeq 2\rho_+\epsilon(2-\epsilon)/\ell^2$, and we can neglect the second order term in ρ_+ . In order to find the Hawking temperature, we now make use of the equation

$$\lim_{\epsilon \rightarrow 0} \text{Im} \frac{1}{\rho - \rho_+ \pm i\epsilon} = \delta(\rho - \rho_+), \quad (69)$$

in this way we find

$$\text{Im} R_\pm = \pm \frac{\tilde{E}\pi}{\mathcal{F}'(\rho)|_{\rho=\rho_+}}, \quad (70)$$

where $\tilde{E} = E + qA_t$. Using $p_\rho^\pm = \pm \partial_\rho R_\pm$, for the total tunneling rate we get

$$\begin{aligned} \Gamma &= \exp\left(\frac{1}{\hbar} \text{Im}(\tilde{E}\Delta t^{\text{out, in}}) - \frac{1}{\hbar} \text{Im} \oint p_\rho d\rho\right) \\ &= \exp\left(-\frac{4\tilde{E}\pi}{\mathcal{F}'(\rho)|_{\rho=\rho_+}}\right). \end{aligned} \quad (71)$$

In the last equation we have also added a temporal part contribution due to the connection of the interior region and the exterior region of the spacetime metric via $t \rightarrow t - i\pi/\mathcal{F}'(\rho)$. Finally, one can obtain the Hawking temperature once we use the Boltzmann factor $\Gamma = \exp(-\tilde{E}/T_H)$, and setting \hbar to unity. That results with

$$T_H = \frac{\mathcal{F}'(\rho)|_{\rho=\rho_+}}{4\pi} = \frac{(2-\epsilon)\epsilon\rho_+}{2\pi\ell^2} = \frac{\epsilon\rho_+}{2\pi R_{\text{AdS}}^2}. \quad (72)$$

This result in terms of charge can be rewritten as

$$T_H = \left(1 + \frac{Q^2}{Q_{\text{ext}}^2}\right) \frac{\epsilon\rho_+}{2\pi\ell^2}. \quad (73)$$

In the case of an extremal black hole $\epsilon\rho_+ \rightarrow 0$, which means that $T_H = 0$. While if $\epsilon\rho_+ = R_{\text{AdS}}$ is different from zero, we get $T_H = 1/(2\pi R_{\text{AdS}})$.

1. A thermal-like nature of Schwinger effect

The spontaneous discharge of the black hole is a result of Hawking radiation and the Schwinger effect. Although the Schwinger effect is not thermal in nature, we would like to elaborate more a possible link and analogy between Hawking radiation and the Schwinger effect in our spacetime geometry. Let us use the Schwinger tunneling rate given by Eq. (61), and rewrite it as follows

$$\Gamma_S \sim \exp\left(-\frac{\pi m_{\text{eff}}^2}{q\mathcal{E}} + \text{corrections}\right), \quad (74)$$

In addition, let us assume that $\mathcal{E} = \mathcal{E}_{\text{local}}$ is some local measured electric field, then we further assume a Boltzmann factor $\Gamma = \exp(-m_{\text{eff}}/T_S)$, i.e., we may write a thermal-like temperature, which is found to be

$$T_S \sim \frac{q\mathcal{E}}{\pi m_{\text{eff}}}, \quad (75)$$

in units $c = \hbar = k_B = 1$. Since $q\mathcal{E} = m_{\text{eff}}a$, where a is some proper accelerations, we get

$$T_S \sim \frac{a}{\pi} \sim 2T_U \quad (76)$$

where we used the relation for the Unruh-like temperature $T_U = a/(2\pi)$. This relation in some sense shows that the thermal-like temperature T_S can be viewed as a Unruh-like temperature. Note that this is just an analogy and the correspondence is not exact. On the other hand, we can write the Hawking temperature given by Eq. (72) in terms of surface gravity

$$T_H = \frac{\kappa}{2\pi}, \quad (77)$$

where $\kappa = \epsilon\rho_+/R_{\text{AdS}}^2$, along with the relation $\kappa = a\sqrt{-g_{tt}}$. From the condition $T_S \sim 2T_H$, we get

$$\frac{q\mathcal{E}\sqrt{-g_{tt}}}{\pi m_{\text{eff}}} = \frac{\epsilon\rho_+}{\pi R_{\text{AdS}}^2}, \quad (78)$$

where, viewed from this coordinate system, we need to use the redshift factor for electric field $\mathcal{E} \rightarrow \mathcal{E}\sqrt{-g_{tt}}$, hence we get

$$\frac{q}{m_{\text{eff}}}\mathcal{E} = \frac{1}{R_{\text{AdS}}}. \quad (79)$$

In this way we obtain the critical temperature

$$T_U = \frac{q}{2\pi m_{\text{eff}}}\mathcal{E} = \frac{1}{2\pi R_{\text{AdS}}}. \quad (80)$$

The condition $T_U \geq 1/(2\pi R_{\text{AdS}})$, onset the Schwinger instability and shows that the pair production is triggered when the Unruh-like temperature exceeds the local AdS curvature scale.

This thermal-like form highlights the interplay between near-horizon acceleration (Unruh temperature) and tunneling suppression. The electric field plays a dual role: it lowers the tunneling barrier, facilitating pair production, but also modifies the near-extremality threshold ϵ_{crit} , beyond which backreaction becomes important [33, 46, 47].

V. A HEURISTIC QUANTUM GRAVITY ARGUMENT

The Hawking temperature associated with the near-extremal black hole geometry, as given in Eq. (72), implies that the black hole will eventually evaporate completely after a sufficiently long time (the evaporation time). On the other hand, the Schwinger temperature derived from Eq. (76) increases without bound as the electric field strength grows, i.e., $T_S \rightarrow \infty$ as $\mathcal{E} \rightarrow \infty$.

A possible resolution to this apparent inconsistency is to consider quantum gravitational effects, particularly those arising from generalized uncertainty principles (GUP), which suggest that [48]

$$\Delta x \geq \frac{\hbar}{\Delta p} + \alpha_0 l_{\text{Pl}}^2 \frac{\Delta p}{\hbar} \quad (81)$$

where l_{Pl} is the Planck length and α_0 some parameter. Solving for Δp we get

$$\frac{\Delta p}{\hbar} \sim \frac{\Delta x}{2\alpha_0 l_{\text{Pl}}^2} \left(1 - \sqrt{1 - \frac{4\alpha_0 l_{\text{Pl}}^2}{\Delta x^2}}\right). \quad (82)$$

The last equation suggests the existence of the minimal length which is proportional to Planck length and can be found from the condition

$$1 - \frac{4\alpha_0 l_{\text{Pl}}^2}{\Delta x_{\text{min}}^2} = 0 \longrightarrow \Delta x_{\text{min}} = 2\sqrt{\alpha_0} l_{\text{Pl}}. \quad (83)$$

Going back to the Hawking temperature (and we set $\hbar = c = 1$) which can be written as

$$T_H = \frac{\epsilon\rho_+}{2\pi R_{\text{AdS}}^2} \sim \frac{\Delta E}{2\pi}, \quad (84)$$

where $\Delta E = \Delta p$ and we can define the lengthscale $\Delta x = R_{\text{AdS}}^2/\epsilon\rho_+$. The modified Hawking temperature can be therefore proposed (with the calibration factor 2π similar to [49]) as follows

$$T_H^{\text{GUP}} = \frac{\Delta x}{4\pi\alpha_0 l_{\text{Pl}}^2} \left(1 - \sqrt{1 - \frac{4\alpha_0 l_{\text{Pl}}^2}{\Delta x^2}}\right) + C \quad (85)$$

where, compared to [49], we have added a constant C which can be fixed from the condition of vanishing Hawking temperature, i.e., $T_H^{\text{GUP}} = 0$, in the limit $\Delta x = \Delta x_{\text{min}}$. The presence of this constant in our view is related to the backreaction effect that arises from the spacetime geometry itself. Fixing the constant we obtain

$$T_H^{\text{GUP}} = \frac{\Delta x}{4\pi\alpha_0 l_{\text{Pl}}^2} \left(1 - \sqrt{1 - \frac{4\alpha_0 l_{\text{Pl}}^2}{\Delta x^2}}\right) - \frac{\Delta x_{\text{min}}}{4\pi\alpha_0 l_{\text{Pl}}^2}. \quad (86)$$

In particular we obtain

$$T_H^{\text{GUP}} = \frac{R_{\text{AdS}}^2}{4\pi\alpha_0 l_{\text{Pl}}^2 \epsilon\rho_+} \left(1 - \sqrt{1 - \frac{4\alpha_0 l_{\text{Pl}}^2 \epsilon^2 \rho_+^2}{R_{\text{AdS}}^4}}\right) - \frac{\Delta x_{\text{min}}}{4\pi\alpha_0 l_{\text{Pl}}^2}. \quad (87)$$

Thus, in the final stage, quantum gravity effect predicts a black hole remnant where Hawking radiation vanishes in the regime

$$\frac{R_{\text{AdS}}^2}{\epsilon \rho_+} \sim l_{\text{Pl}}. \quad (88)$$

Finally, if we perform a series expansion around Planck length in leading order terms we get

$$T_H^{\text{GUP}} = \frac{\epsilon \rho_+}{2\pi R_{\text{AdS}}^2} - \frac{1}{2\pi \sqrt{\alpha_0} l_{\text{Pl}}} + \mathcal{O}(l_{\text{Pl}}^2). \quad (89)$$

The first term matches our result in Eq. (72); however, the additional term (second term) can be interpreted as a backreaction effect that arises from the spacetime geometry. Such a BTZ spacetime metric geometry with minimal length effect was obtained in [50].

Let us now apply these ideas to the Schwinger-like temperature which results in

$$T_S = \frac{q}{\pi m_{\text{eff}}} \mathcal{E} \sim \frac{\Delta E}{\pi}, \quad (90)$$

where we can define again the lengthscale $\Delta x = m_{\text{eff}}/(q\mathcal{E})$. In this case we propose the following relation

$$T_S^{\text{GUP}} = \frac{\Delta x}{4\pi \alpha_0 l_{\text{Pl}}^2} \left(1 - \sqrt{1 - \frac{4\alpha_0 l_{\text{Pl}}^2}{\Delta x^2}} \right) + C. \quad (91)$$

Again, by construction, we can fix the constant C from the vanishing Schwinger-like temperature. In addition, from the last equation we see that it leads to the condition

$$\Delta x_{\text{min}} = 2\sqrt{\alpha_0} l_{\text{Pl}} = m_{\text{eff}}/(q\mathcal{E}_{\text{crit}}), \quad (92)$$

in other words, it suggesting the existence of a critical electric field given by

$$\mathcal{E}_{\text{crit}} = \frac{m_{\text{eff}}}{2q\sqrt{\alpha_0} l_{\text{Pl}}}. \quad (93)$$

The last equation shows a connection between the electric field and the minimal length, which, to the best of our knowledge, has not been reported before. Finally, for the Schwinger-like temperature we have

$$T_S^{\text{GUP}} = \frac{m_{\text{eff}}}{4q\mathcal{E}\pi\alpha_0 l_{\text{Pl}}^2} \left(1 - \sqrt{1 - \frac{4\alpha_0 q^2 \mathcal{E}^2 l_{\text{Pl}}^2}{m_{\text{eff}}^2}} \right) - \frac{m_{\text{eff}}}{2\pi q \mathcal{E}_{\text{crit}} \alpha_0 l_{\text{Pl}}^2}. \quad (94)$$

Therefore, the Schwinger-like temperature vanishes when the electric field reaches its maximum value, $\mathcal{E} = \mathcal{E}_{\text{crit}}$. Owing to the existence of a minimal length scale, as implied by the generalized uncertainty principle, we argue that this effect can resolve the apparent paradox and

prevent the divergence of the Schwinger-like temperature. Finally, by performing a series expansion around the Planck length, we obtain

$$T_S^{\text{GUP}} = \frac{q}{\pi m_{\text{eff}}} \mathcal{E} - \frac{1}{2\pi \sqrt{\alpha_0} l_{\text{Pl}}} + \mathcal{O}(l_{\text{Pl}}^2), \quad (95)$$

where the first term matches Eq. (76), while the second term is again due to the backreaction effect that arises from the spacetime geometry itself (like the solution in [50]).

VI. QUANTUM ENTROPY AND THE NEAR-HORIZON BTZ GEOMETRY

In Section III, we explored semiclassical instability via the Schwinger effect, finding that pair production concentrates near the extremal surface. We now complement this analysis by turning to the quantum structure of the near-horizon geometry, using both geometric extremization and operator algebra. This approach reveals how the same region of spacetime—where instability emerges—is also where quantum entropy localizes, modular energy flux peaks, and von Neumann algebras acquire physical meaning.

A. Geometry of Near-Extremal BTZ and the Expansion in ϵ

The BTZ solution in 2 + 1 dimensions offers a striking laboratory to explore quantum corrections. In its extremal limit, the black hole temperature drops to zero and the inner and outer horizons coincide. Remarkably, the near-horizon region does not become trivial—it develops a long AdS_2 throat that governs the infrared physics of the system. This emergent structure provides an ideal setting for applying the quantum entropy functional (QEF) formalism and exploring its deeper algebraic implications.

To isolate the throat geometry, we perform a near-horizon and near-extremal expansion, as introduced in Section III. We parametrize the radial coordinate as (22) where r_e is the extremal horizon radius and $\epsilon \ll 1$ is a small deviation from extremality. Furthermore, we can switch to ingoing null coordinate U using

$$U = T + \int \frac{d\rho}{f(\rho)}, \quad (96)$$

the BTZ metric becomes:

$$ds^2 = -\frac{2-\epsilon}{\ell^2} \rho^2 dU^2 + 2 dU d\rho + r_e^2 d\phi^2, \quad (97)$$

where U is the ingoing Eddington–Finkelstein coordinate and ℓ is the AdS_3 radius. This describes an $\text{AdS}_2 \times S^1$ throat geometry, with AdS_2 radius given by (40). As $\epsilon \rightarrow 0$, we recover the pure extremal geometry with

$R_2^2 = \ell^2/2$. This form of the metric makes manifest the emergence of a long AdS_2 throat near the extremal horizon. The parameter ϵ controls the proper length of the throat, and as $\epsilon \rightarrow 0$ the geometry asymptotes to an infinitely long AdS_2 region. This behavior is typical of extremal black holes and signals the decoupling of infrared physics, a feature that underlies the $\text{AdS}_2/\text{CFT}_1$ correspondence.

In what follows, we primarily work in ingoing Eddington–Finkelstein coordinates, adapted to the past horizon \mathcal{H}^- . This choice simplifies the analysis of modular flow and gravitationally dressed observables in Section VII. Since the near-extremal BTZ geometry retains a bifurcate Killing horizon even in the near-horizon limit, the same formalism applies symmetrically to the future horizon \mathcal{H}^+ when the system is prepared in a time-symmetric state, such as the Hartle–Hawking vacuum. In this limit, the relevant extremal surfaces are not boundary-anchored geodesics crossing only \mathcal{H}^+ , but instead lie near the bifurcation point, where the variation of generalized entropy vanishes. This region captures the semiclassical balance between area and entanglement entropy, and coincides with the peak of Schwinger pair production and modular energy flux across both horizons.

B. The Quantum Entropy Function and One-Loop Corrections

What happens to the entropy of a black hole when quantum fields are allowed to fluctuate in its vicinity? The classical Bekenstein–Hawking formula tells us that entropy is proportional to the area of the event horizon, but this relation is incomplete. In semiclassical gravity, where quantum fields propagate on curved spacetimes, quantum corrections appear—encoding subtle entanglement effects near the horizon. Understanding these corrections is essential for unraveling the microstructure of spacetime.

One of the most powerful and systematic frameworks for computing such corrections is the *quantum entropy function* (QEF) formalism introduced by Sen [19, 20]. This method is tailored for extremal black holes, whose near-horizon geometries exhibit a universal AdS_2 throat. The Euclidean continuation becomes a warped product

$$\text{AdS}_2 \times \mathcal{K}, \quad (98)$$

where \mathcal{K} is a compact transverse space capturing angular or internal directions. The central idea is to evaluate the Euclidean path integral over this background:

$$d_{\text{micro}} = \int \mathcal{D}\Phi e^{-I_{\text{eff}}[\Phi]}, \quad (99)$$

with Φ denoting all fluctuating fields and I_{eff} the effective action.

At one-loop order, the dominant correction arises from Gaussian fluctuations, yielding a determinant of the ki-

netic operator:

$$S_{1\text{-loop}} = -\frac{1}{2} \log \det \Delta. \quad (100)$$

For a minimally coupled scalar, this is the Laplacian determinant on $\text{AdS}_2 \times \mathcal{K}$, computable via heat kernel or zeta function techniques [20, 24, 25].

In the near-horizon geometry derived above, the one-loop entropy correction becomes:

$$S_{1\text{-loop}} = -\frac{1}{2} \log \left(\frac{A}{2\pi(2-\epsilon)G} \right), \quad (101)$$

where $A = 2\pi r_e$ is the extremal horizon circumference. This captures both the universal logarithmic correction and smooth deviations from extremality.

This logarithmic term dominates in the extremal limit and encodes the leading quantum correction due to massless matter fields. It reflects the entanglement of near-horizon quantum excitations and is robust under regularization choices. As we will see in Section VII, this entropy admits a deeper operator-theoretic interpretation: it arises from a trace over a semifinite von Neumann algebra of gravitationally dressed observables localized on the black hole horizon.

VII. VON NEUMANN ALGEBRAS AND THE MODULAR HAMILTONIAN

We now formulate the semiclassical entropy of the near-extremal charged BTZ black hole within the rigorous framework of operator algebras and modular theory. Following the algebraic formalism of Tomita–Takesaki theory [51, 52], and incorporating gravitational dressing and quantum flux, we demonstrate that the generalized black hole entropy is precisely a von Neumann entropy defined on a Type II_∞ von Neumann algebra of horizon observables.

Let \mathcal{H} be a Hilbert space and $\mathcal{A} \subset \mathcal{B}(\mathcal{H})$ a von Neumann algebra of bounded operators acting on \mathcal{H} . We consider a cyclic and separating vector $\Omega \in \mathcal{H}$ such that:

- **Cyclic:** The set $\mathcal{A}\Omega$ is dense in \mathcal{H} ,
- **Separating:** $A\Omega = 0$ implies $A = 0$ for all $A \in \mathcal{A}$.

This triple $(\mathcal{A}, \mathcal{H}, \Omega)$ defines the standard Tomita–Takesaki modular theory, which associates to each such triple a modular operator Δ , modular conjugation J , and modular automorphism group $\sigma_t(A) = \Delta^{it} A \Delta^{-it}$. The vector state $\omega(A) = \langle \Omega, A\Omega \rangle$ satisfies the KMS condition with respect to σ_t , providing a thermal characterization of modular flow [36, 53].

In the presence of gravity, the relevant algebra $\mathcal{A}_{\mathcal{H}^-}^{\text{grav}}$ admits a semifinite trace due to the Type II_∞ structure identified in [54], allowing a finite modular Hamiltonian and entropy to be defined. The modular flow generated by the vector field $\xi = 2\pi U \partial_U$ is implemented by σ_t on this algebra, and governs the quantum evolution along the horizon.

A. Quantum Modular Flux and Gravitational Backreaction

We consider scalar field Φ with mass m and charge q , minimally coupled to a fixed background gauge field A_μ . The field satisfies the covariant Klein-Gordon equation (20). The near-horizon, near-extremal geometry of the charged BTZ black hole is given by (13) where $\epsilon \ll 1$ controls the deviation from extremality, and the gauge field (18) has the near-horizon behavior so that $A_U \rightarrow 0$ on the horizon.

The classical phase space \mathcal{P} consists of solutions Φ to the above equation. It carries the symplectic structure [55–57]:

$$\mathcal{W}(\Phi_1, \Phi_2) = \int_{\Sigma} d\Sigma^\mu \text{Im}(\Phi_1^* D_\mu \Phi_2), \quad (102)$$

which reduces on the past horizon \mathcal{H}^- to

$$\mathcal{W}_{\mathcal{H}^-}(\Phi_1, \Phi_2) = \int dU d\phi r_e \cdot \text{Im}(\Phi_1^* \partial_U \Phi_2). \quad (103)$$

This horizon phase space is the natural setting for defining the modular Hamiltonian generator of boost flow [58, 59]. For the boost Killing vector $\xi = \partial_U$, the modular flux is defined by

$$F^{\mathcal{H}}\xi = \mathcal{W}\mathcal{H}^-(\Phi, \mathcal{L}\xi\Phi) = \int dU d\phi r_e \cdot \text{Im}(\Phi^* \partial_U \Phi). \quad (104)$$

This flux appears as the expectation value of the modular Hamiltonian in an excited state and captures the backreaction from Schwinger pair production.

This expression is closely related to the stress-energy component $T_{UU} \approx |\partial_U \Phi|^2$ near the horizon, as derived from the action. Thus, the modular flux directly reflects the energy carried by quantum excitations of the scalar field across the horizon.

By symmetry and conservation laws, this modular energy flux must be balanced by a gravitational response. The gravitational charges on the horizon satisfy the constraint:

$$\delta^2 Q_+ - \delta^2 Q_- = -4G\beta F_\xi^{\mathcal{H}}, \quad (105)$$

where $\beta = 2\pi/\kappa$ with $\kappa = \frac{2(2-\epsilon)}{\ell^2}$ the surface gravity of the horizon. This equation arises from the Raychaudhuri constraint and determines the semiclassical deformation of the extremal surface.

The quantities $\delta^2 Q_+$ and $\delta^2 Q_-$ correspond to second-order gravitational charges evaluated on null slices of the future and past horizon, respectively. Physically, they capture the integrated backreaction due to the energy flux of the scalar field at late and early times. In our coordinates, they are given by integrals of the stress tensor component T_{UU} as $U \rightarrow \pm\infty$. This connects the algebraic modular flow to the Raychaudhuri constraint in semiclassical gravity.

The full backreaction is encoded in the variation of the generalized entropy:

$$S_{\text{gen}} = \frac{A}{4G} + S_{\text{vN}}, \quad \delta S_{\text{gen}} = \frac{\delta A}{4G} + \beta F^{\mathcal{H}}\xi, \quad (106)$$

and the quantum extremality condition $\delta S_{\text{gen}} = 0$ then yields:

$$\delta A = -4G\beta F_\xi^{\mathcal{H}}. \quad (107)$$

This condition governs the location of the quantum extremal surface and captures the leading semiclassical balance between classical geometry and quantum matter.

Although we compute the modular Hamiltonian K and flux F_ξ on the past horizon \mathcal{H}^- , the time-reflection symmetry of the near-horizon BTZ geometry ensures that the same expressions apply to the future horizon \mathcal{H}^+ . The modular generator $\xi^a = 2\pi U \partial_U^a$ maps under Killing reflection to $\xi^a = -2\pi V \partial_V^a$, preserving the form of the flux integral. This justifies using F_ξ as a symmetric observable across the bifurcation surface. In this formulation, we do not split the flux into "quantum" and "gravitational" parts, but rather compute it canonically via the symplectic pairing and relate it directly to geometric backreaction through the constraint equation above. This approach unifies the algebraic definition of entropy with its gravitational realization in semiclassical spacetime.

In the next section, we show how this modular energy flux manifests geometrically: the same location that extremizes S_{gen} also marks the intersection of inward and outward RT geodesics—providing a unified picture where modular flow, entropy variation, and holographic geometry all converge.

In our semiclassical framework, the appearance of the second variation $\delta^2 T_{UU}$ in the modular flux and gravitational constraint is not ad hoc, but a natural consequence of quantum field theory in curved spacetime. In classical general relativity, the Einstein equations relate the curvature tensor directly to the stress-energy tensor of classical matter fields. However, when quantum matter is coupled to a classical background geometry, the stress-energy tensor becomes an operator-valued distribution. The semiclassical Einstein equation takes the form

$$R_{ab} - \frac{1}{2}Rg_{ab} + \Lambda g_{ab} = 8\pi G\langle T_{ab} \rangle, \quad (108)$$

where the expectation value $\langle T_{ab} \rangle$ is computed in a quantum state of the matter fields.

In this setting, we consider a perturbation of the vacuum state—such as that caused by Schwinger pair production—and expand the expectation value of the stress tensor as

$$\langle T_{ab} \rangle = T_{ab}^{(0)} + \delta T_{ab}^{(1)} + \delta^2 T_{ab}^{(2)} + \dots, \quad (109)$$

where $T_{ab}^{(0)}$ corresponds to the vacuum, $\delta T_{ab}^{(1)}$ vanishes due to symmetry under time reflection in the Hartle-Hawking vacuum, and the first physically meaningful contribution comes from the second-order variation

$\delta^2 T_{ab}$. This is the term that sources modular energy flux and governs the leading-order backreaction on the geometry.

Consequently, the entropy variation $\delta S_{\text{gen}} = 0$ leads to a constraint equation of the form

$$R_{UU} = 4G\beta\delta^2 T_{UU}, \quad (110)$$

which we interpret as the null-null component of the semiclassical Einstein equations, projected along the horizon generator. This is the natural semiclassical generalization of the thermodynamic derivation proposed by Jacobson [35], and reflects how quantum fluctuations induce the gravitational response through modular energy flow. We now explicitly derive the null-null component of the semiclassical Einstein equations from the variation of the generalized entropy. The variation of the generalized entropy is given by

$$\delta S_{\text{gen}} = \frac{\delta A}{4G} + \beta F_\xi, \quad (111)$$

where δA is the variation of the horizon area and F_ξ is the modular Hamiltonian flux across the past horizon \mathcal{H}^- , canonically defined as

$$F_\xi = \int_{\mathcal{H}^-} dU d\phi \xi^U(U) \delta^2 T_{UU}(U, \phi). \quad (112)$$

To express δA in terms of the curvature, we let $A(\lambda)$ be the area of a cross-sectional slice of a bundle of null generators along affine parameter λ , with tangent vector $\xi^a = \frac{d}{d\lambda} = \partial_U$. The evolution of $A(\lambda)$ is governed by the Raychaudhuri equation [60]:

$$\frac{d\theta}{d\lambda} = -\frac{1}{2}\theta^2 - \sigma_{ab}\sigma^{ab} - R_{ab}\xi^a\xi^b. \quad (113)$$

Integrating once with respect to $\lambda = U$ yields the area variation:

$$\delta A = - \int dU d\phi U R_{UU} r_e. \quad (114)$$

On the other hand, the modular flux in the same coordinates is given by

$$F_\xi = 2\pi \int dU d\phi U \delta^2 T_{UU} r_e. \quad (115)$$

Substituting both δA and F_ξ into the entropy variation equation, we obtain:

$$\begin{aligned} \delta S_{\text{gen}} = & -\frac{1}{4G_N} \int dU d\phi U R_{UU} r_e \\ & + \beta \int dU d\phi U \delta^2 T_{UU} r_e. \end{aligned} \quad (116)$$

Factoring out the common integral, we have:

$$\delta S_{\text{gen}} = \int dU d\phi U r_e \left(-\frac{R_{UU}}{4G} + \beta \delta^2 T_{UU} \right). \quad (117)$$

Demanding $\delta S_{\text{gen}} = 0$ for arbitrary perturbations implies that the integrand must vanish pointwise, yielding the constraint:

$$R_{UU} = 4G\beta\delta^2 T_{UU}. \quad (118)$$

This is precisely the null-null component of the semiclassical Einstein equation, projected along the horizon generator $\xi^a = \partial_U$. It expresses how quantum energy flux across the horizon induces curvature, derived purely from horizon entropy flow and modular Hamiltonian considerations.

B. Geodesic RT Surfaces and Semiclassical Entropy

To visualize this balance, we turn to spacelike geodesics in the near-horizon BTZ geometry. On a constant- T slice, the induced spatial metric is:

$$ds_{\text{slice}}^2 = \frac{\ell^2}{(2-\epsilon)\rho^2} d\rho^2 + r_e^2 d\phi^2. \quad (119)$$

We consider extremal surfaces parameterized by $\rho(\phi)$, anchored on the asymptotic boundary. The Ryu–Takayanagi (RT) length functional becomes:

$$\mathcal{L}[\rho(\phi)] = \int d\phi \sqrt{\frac{\ell^2}{(2-\epsilon)\rho^2} \left(\frac{d\rho}{d\phi} \right)^2 + r_e^2}. \quad (120)$$

A natural class of geodesics takes the exponential form $\rho(\phi) = \rho_0 e^{\kappa\phi}$, where κ encodes the angular momentum L , so that the RT entropy becomes:

$$S_{\text{RT}} = \frac{\Delta\phi \cdot r_e^2}{4GL}. \quad (121)$$

In the circular limit we recover the Bekenstein–Hawking result:

$$S_{\text{BH}} = \frac{\pi r_e}{2G}. \quad (122)$$

Here, geometry reveals its quantum hand. RT surfaces—geodesics derived from area minimization—spiral inward and outward from boundary intervals and intersect precisely in the region where Schwinger pair production becomes dominant. The saddle point of tunneling matches the extremal surface in the entanglement wedge. It is as if the geometry “anticipated” the quantum process from the outset.

This coincidence is not accidental: the location where the RT geodesics intersect also marks the concentration of modular energy flux $F_\xi^{\mathcal{H}}$ computed in the previous section. From the perspective of operator algebra, this is where the modular Hamiltonian generates maximal entanglement flow across the horizon. Geometrically, it is where the entanglement wedge “pinches,” and physically, it is where the gravitational backreaction from pair production becomes significant. The intersection of inward

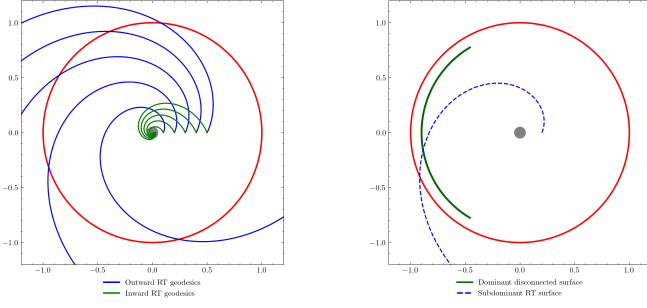


FIG. 3: **(a)** In the small interval limit, inward (green) and outward (blue) RT geodesics intersect near the horizon, forming a connected extremal surface. **(b)** For large intervals, disconnected RT surfaces dominate. The red curve is the asymptotic boundary; the gray dot marks the black hole center.

and outward RT geodesics near the bifurcation point is not merely a geometric feature—it signals the onset of significant quantum effects. In particular, the saddle region where these geodesics pinch corresponds to the locus of maximal Schwinger pair production in the near-horizon electric field. This pair production process, triggered by the background gauge field, generates entangled particles that cross opposite horizons: one escapes through \mathcal{H}^+ , contributing to the entanglement entropy of the exterior region, while the other falls inward across \mathcal{H}^- . The quantum extremal surface, where the variation of generalized entropy vanishes, lies precisely at this junction, unifying holographic geometry, quantum field theory, and modular dynamics in a single causal structure. To complement the top-down geodesic perspective, we now turn to the causal structure of the near-horizon region. In the Penrose diagram shown below, the bifurcate Killing horizon of the near-extremal BTZ black hole provides a natural setting to visualize both the quantum extremal surface and the dynamics of Schwinger pair production. The red RT surface represents a space-like extremal surface localized near the bifurcation point, consistent with the emergence of a long AdS_2 throat in the near-extremal limit. This surface is the geometric manifestation of the quantum extremal surface defined by $\delta S_{\text{gen}} = 0$. As shown earlier, this condition implies $\delta A = -4G_N \beta F_\xi^{\mathcal{H}}$, balancing classical area variation with modular energy flux. The geodesic extremization in this region is therefore not only a minimal-area condition—it also encodes the modular dynamics of the horizon algebra. This surface is not anchored to boundary intervals, but instead captures the local extremal condition $\delta S_{\text{gen}} = 0$, where the classical area and modular energy flux are precisely balanced. The pair production process peaks in this region, with the entangled particles escaping across opposite horizons, thereby contributing to the semiclassical entropy flow. *The geometry doesn't just "know" where particles will go — it is the quantum information that defines their behavior.* Finally, we in-

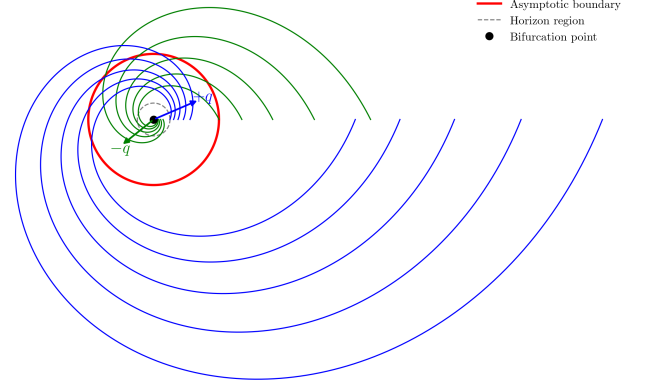


FIG. 4: RT geodesics and Schwinger pair production near the bifurcation point. In this top-down view of the near-horizon BTZ geometry, inward (green) and outward (blue) RT geodesics intersect near the origin, forming a connected extremal surface. At the intersection point—the quantum extremal surface—a charged particle-antiparticle pair is produced via the Schwinger effect. The positively charged particle escapes across the future horizon \mathcal{H}^+ , while its negatively charged partner falls inward across \mathcal{H}^- . This region marks the peak of modular energy flux and the vanishing of δS_{gen} , where semiclassical entropy variation is extremized.

corporate quantum corrections via the one-loop entropy (101) from Section VI.

The full semiclassical entropy becomes:

$$S_{\text{gen}} = \frac{A}{4G} - \frac{1}{2} \log \left(\frac{A}{4\pi G} \right) - \frac{\epsilon}{4} + \dots \quad (123)$$

This expression unites all elements of the theory: classical geometry, holographic entanglement, quantum fluctuations, and algebraic structure. The quantum extremal surface is where the entanglement wedge closes, pair production peaks, and entropy variations cancel—a testament to the harmony between spacetime and information.

The intersection point of the inward (green) and outward (blue) RT geodesics near the horizon corresponds to the location where the extremal surface “pinches,” marking the saddle of the minimal surface in the entanglement wedge. Remarkably, this location also coincides with the region where the modular energy flux from Schwinger pair production becomes dominant. The emergence of this common region is not coincidental—it signals a deep interplay between the geometry of entanglement and the dynamics of quantum field theory in curved spacetime. The quantum extremal surface “knows” where entropy variation vanishes, and this is precisely where pair production concentrates. The geometry doesn’t just passively encode quantum matter—it anticipates it through the structure of extremal surfaces. In our near-extremal, near-horizon charged BTZ geome-

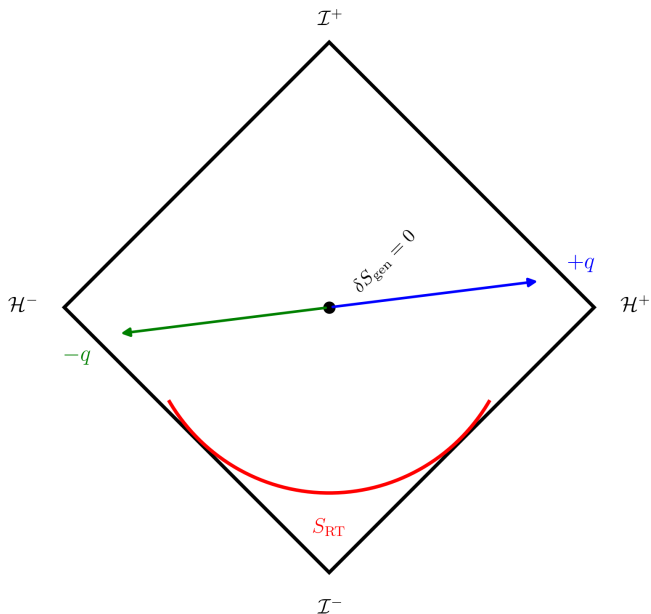


FIG. 5: Penrose diagram of Schwinger pair production and quantum extremal surface. The near-horizon geometry admits a bifurcate Killing horizon, with past and future horizons \mathcal{H}^- and \mathcal{H}^+ . The red arc represents a local RT surface centered near the bifurcation point, satisfying the quantum extremality condition $\delta S_{\text{gen}} = 0$.

At this location, a charged pair is produced by the Schwinger effect: the positive-charge particle escapes across \mathcal{H}^+ , while its negative partner falls inward across \mathcal{H}^- .

try, we expand the coordinates as $r = r_e + \epsilon\rho$ and $t = T/\epsilon$, where $\epsilon \ll 1$ parametrizes the deviation from extremality. The lapse function becomes $f(r) \approx \frac{(2-\epsilon)}{\ell^2} \epsilon^2 \rho^2$, implying that the Hawking temperature scales as $T \sim \epsilon/\ell^2$. Meanwhile, the Bekenstein–Hawking entropy expands as $S_{\text{BH}} = \pi r_e/2G_N + \pi\epsilon/2G_N$, so that $\delta S \sim \epsilon \sim T$. Applying the first law $\delta E = T\delta S$, we obtain:

$$\delta E \sim \frac{T^2}{G}, \quad (124)$$

which exactly matches the scaling relation $\delta E \sim T^2/M_{\text{gap}}$ discussed in [43, 54]. Although a full spectral analysis (e.g., via partition function and Laplace transform) is needed to confirm continuity, our smooth semiclassical expansion already supports the absence of a mass gap in the charged BTZ case, analogous to the Reissner–Nordström scenario. Based on this behavior, we do not expect a mass gap to arise in this setup either. The Schwinger effect and the von Neumann entropy are intimately connected through the dynamics of vacuum fluctuations in curved spacetime. In our setup, charged scalar particles are spontaneously produced near the horizon due to the background electric field and gravitational potential, as described by the Klein–Gordon equation. Each pair production event creates an entangled particle–

antiparticle pair, with one particle escaping to the boundary and the other falling into the black hole. This process effectively transfers quantum information across the horizon, modifying the field state and introducing correlations between accessible and inaccessible regions. As a result, the reduced density matrix becomes mixed, and its von Neumann entropy increases. The same field modes responsible for the Schwinger flux F_{ξ}^{quantum} generate the modular Hamiltonian and define the algebra $\mathcal{A}_{\mathcal{H}^-}^{\text{grav}}$ on which the entropy is computed. Thus, pair production not only populates the entanglement wedge but also furnishes the observables through which its informational content is measured, linking the physical process of particle creation to the operator-algebraic structure of black hole entropy.

These observables live in the von Neumann algebra $\mathcal{A}_{\mathcal{H}^-}^{\text{grav}}$, whose modular Hamiltonian defines the flux $F_{\xi}^{\mathcal{H}}$. Thus, the geodesic extremal surface is not just a geometric boundary—it also defines the domain on which operator algebra dynamics and gravitational backreaction are co-encoded in semiclassical gravity.

VIII. DISCUSSION AND OUTLOOK

The near-horizon region of a near-extremal charged BTZ black hole provides a unique possibility for exploring the intersection of semiclassical gravity, quantum field theory, and operator algebra in a profoundly instructive regime.

In this work, we obtained a near-horizon geometry of a near-extremal BTZ black hole. We then analyzed the propagation of the charged scalar field in a warped $\text{AdS}_2 \times S^1$ geometry supported by a constant background electric field. This setup naturally realizes the Schwinger effect [29–31, 33, 34], where entangled particle–antiparticle pairs are spontaneously created near the bifurcation surface. But we went further: by solving the Klein–Gordon equation in this background, we also described the Hawking radiation of charged particles as a tunneling process. The near-horizon WKB analysis showed that the Hawking temperature arises from the imaginary part of the classical action, via quantum tunneling. This semiclassical radiation is governed by both the local electric field and the redshifted geometry, giving rise to a thermal spectrum with a temperature that vanishes in the extremal limit. We also pointed out the thermal-like nature of the Schwinger effect.

Yet the most striking insight emerges when the generalized uncertainty principle is applied. We argued that quantum gravity effects imply the existence of a minimal length and, importantly, can lead to the vanishing of both the Hawking and Schwinger-like temperatures. As a result, the final stage of Hawking and Schwinger evaporation may be a stable black hole remnant.

By examining the modular Hamiltonian flux associated with outgoing radiation, we showed that the Schwinger and Hawking effects are not just processes within space–

time—they are imprinted on its geometry. The variation of the generalized entropy, which includes both the area term and the modular energy flux, vanishes precisely where pair production is most intense. This identifies the quantum extremal surface not as an abstract construct, but as the locus where gravitational and quantum contributions balance each other. Using a second-order perturbative expansion of the stress-energy tensor, we derived the null-null component of the semiclassical Einstein equations directly from the condition $\delta S_{\text{gen}} = 0$. This shows that gravitational curvature is sourced by the quantum flux across the horizon—an elegant semiclassical realization of Jacobson’s idea that Einstein’s equations can be viewed as an equation of state arising from entropy flow [35].

What gives this entire framework its mathematical rigor is the operator-algebraic structure underpinning horizon observables. We worked within the von Neumann algebra of gravitationally dressed operators on the horizon, showing that it forms a Type II_∞ algebra with a well-defined trace. This allowed us to define modular Hamiltonians, entropy, and energy flux in a UV-finite, state-independent manner. Using the tools of Tomita–Takesaki theory [36, 37, 39, 51, 52], we interpreted modular flow as a dynamical process that encodes not only entanglement but also the backreaction of quantum matter on geometry.

The central geometric signature of this interplay is the point where inward and outward Ryu–Takayanagi (RT) geodesics intersect—precisely the region where entropy variation vanishes and pair production peaks. This is not a coincidence; it is a manifestation of the deep alignment between holographic surfaces, modular energy, and quantum instability. The near-horizon geometry doesn’t just respond to quantum matter—it anticipates and organizes it.

Several exciting issues remain open. One is to extend this analysis to dynamical spacetimes—those undergoing evaporation, infall, or collapse—where modular flow becomes time-dependent and the balance of entropy and flux evolves dynamically. Another is to explore higher-dimensional black holes, where horizon topology and causal structure offer new terrain for entanglement and operator algebra. The broader lesson is that black hole interiors, quantum radiation, and entanglement entropy are not separate threads—they are aspects of a single, underlying structure. By tracing modular flux, entropy variation, and particle production to a common geometric and algebraic origin, we begin to see a more complete picture: one in which the black hole horizon is not just a boundary, but a site of profound quantum organization. Geometry, in this view, doesn’t merely react to quantum fields—it predicts where they appear, how they evolve, and how they encode information.

-
- [1] S. W. Hawking, *Commun. Math. Phys.* **43**, 199 (1975), [Erratum: *Commun.Math.Phys.* 46, 206 (1976)].
 - [2] W. G. Unruh, *Phys. Rev. D* **14**, 870 (1976).
 - [3] D. N. Page, *Phys. Rev. D* **13**, 198 (1976).
 - [4] J. D. Bekenstein, *Phys. Rev. D* **7**, 2333 (1973).
 - [5] S. W. Hawking, *Phys. Rev. D* **13**, 191 (1976).
 - [6] S. Das, P. Majumdar, and R. K. Bhaduri, *Class. Quant. Grav.* **19**, 2355 (2002), [arXiv:hep-th/0111001](#).
 - [7] M. K. Parikh and F. Wilczek, *Phys. Rev. Lett.* **85**, 5042 (2000), [arXiv:hep-th/9907001](#).
 - [8] M. Banados, C. Teitelboim, and J. Zanelli, *Phys. Rev. Lett.* **69**, 1849 (1992), [arXiv:hep-th/9204099](#).
 - [9] M. Banados, M. Henneaux, C. Teitelboim, and J. Zanelli, *Phys. Rev. D* **48**, 1506 (1993), [Erratum: *Phys.Rev.D* 88, 069902 (2013)], [arXiv:gr-qc/9302012](#).
 - [10] S. Carlip, *Class. Quant. Grav.* **12**, 2853 (1995), [arXiv:gr-qc/9506079](#).
 - [11] R. R. Poojary, *Phys. Rev. D* **107**, 066019 (2023), [arXiv:2209.03065 \[hep-th\]](#).
 - [12] J. M. Maldacena, *Adv. Theor. Math. Phys.* **2**, 231 (1998), [hep-th/9711200](#).
 - [13] M. Cadoni and S. Mignemi, *Nucl. Phys. B* **557**, 165 (1999), [arXiv:hep-th/9902040](#).
 - [14] A. Almheiri, X. Dong, and D. Harlow, *JHEP* **2015** (04), 163, [1411.7041](#).
 - [15] J. Maldacena, D. Stanford, and Z. Yang, *PTEP* **2016**, 12C104, [1606.01857](#).
 - [16] K. Jensen, *Phys. Rev. Lett.* **117**, 111601 (2016), [1605.06098](#).
 - [17] A. Almheiri, N. Engelhardt, D. Marolf, and H. Maxfield, *JHEP* **12**, 063, [arXiv:1905.08762 \[hep-th\]](#).
 - [18] G. Penington, *JHEP* **09**, 002, [ar:1905.08255](#).
 - [19] A. Sen, *International Journal of Modern Physics A* **24**, 4225 (2009), [arXiv:0809.3304 \[hep-th\]](#).
 - [20] A. Sen, *Journal of High Energy Physics* **2013**, 156 (2013), [arXiv:1205.0971 \[hep-th\]](#).
 - [21] A. Sen, *JHEP* **04**, 156, [arXiv:1205.0971 \[hep-th\]](#).
 - [22] D. V. Fursaev, *Phys. Rev. D* **51**, 5352 (1995), [arXiv:hep-th/9412161](#).
 - [23] V. P. Frolov, D. V. Fursaev, and A. I. Zelnikov, *Nuclear Physics B* **486**, 339 (1997), [arXiv:hep-th/9607104](#).
 - [24] T. Barrella, X. Dong, S. A. Hartnoll, and V. Martin, *Journal of High Energy Physics* **2013**, 109 (2013), [arXiv:1306.4682 \[hep-th\]](#).
 - [25] N. Banerjee, R. K. Gupta, I. Mandal, and A. Sen, *Journal of High Energy Physics* **2011**, 143 (2011), [arXiv:1005.3044 \[hep-th\]](#).
 - [26] T. Faulkner, A. Lewkowycz, and J. Maldacena, *Journal of High Energy Physics* **2013**, 074 (2013), [arXiv:1307.2892 \[hep-th\]](#).
 - [27] A. Lewkowycz and J. Maldacena, *Journal of High Energy Physics* **2013**, 90 (2013), [arXiv:1304.4926 \[hep-th\]](#).
 - [28] T. Faulkner, A. Lewkowycz, and J. Maldacena, *JHEP* **11**, 074, [arXiv:1307.2892 \[hep-th\]](#).
 - [29] J. S. Schwinger, *Phys. Rev.* **82**, 664 (1951).
 - [30] G. W. Gibbons, *Commun. Math. Phys.* **44**, 245 (1975).
 - [31] C.-M. Chen, S. P. Kim, I.-C. Lin, J.-R. Sun, and M.-F. Wu, *Phys. Rev. D* **85**, 124041 (2012), [arXiv:1202.3224 \[hep-th\]](#).
 - [32] C.-M. Chen, J.-R. Sun, F.-Y. Tang, and P.-Y. Tsai, *Class.*

- Quant. Grav. **32**, 195003 (2015), arXiv:1412.6876 [hep-th].
- [33] R.-G. Cai, C.-M. Chen, S. P. Kim, and J.-R. Sun, Phys. Rev. D **101**, 105015 (2020), arXiv:2004.00735 [hep-th].
- [34] C.-M. Chen and S. P. Kim, Phys. Rev. D **101**, 085014 (2020), arXiv:2002.00394 [hep-th].
- [35] T. Jacobson, Phys. Rev. Lett. **75**, 1260 (1995), arXiv:gr-qc/9504004.
- [36] R. Haag, *Local quantum physics: Fields, particles, algebras* (1992).
- [37] E. Witten, JHEP **10**, 008, arXiv:2112.12828 [hep-th].
- [38] V. Chandrasekaran, R. Longo, G. Penington, and E. Witten, JHEP **02**, 082, arXiv:2206.10780 [hep-th].
- [39] V. Chandrasekaran, G. Penington, and E. Witten, JHEP **04**, 009, arXiv:2209.10454 [hep-th].
- [40] S. Ryu and T. Takayanagi, Phys. Rev. Lett. **96**, 181602 (2006), arXiv:hep-th/0603001.
- [41] S. Ryu and T. Takayanagi, JHEP **08**, 045, arXiv:hep-th/0605073.
- [42] V. E. Hubeny, M. Rangamani, and T. Takayanagi, JHEP **07**, 062, arXiv:0705.0016 [hep-th].
- [43] L. V. Iliesiu and G. J. Turiaci, JHEP **05**, 145, arXiv:2003.02860 [hep-th].
- [44] A. Sen, Int. J. Mod. Phys. A **24**, 4225 (2009), arXiv:0809.3304 [hep-th].
- [45] S. P. Kim and D. N. Page, Phys. Rev. D **78**, 103517 (2008), arXiv:0803.2555 [hep-th].
- [46] S. P. Kim, H. K. Lee, and Y. Yoon, Int. J. Mod. Phys. D **28**, 1950139 (2019), arXiv:1503.00218 [hep-th].
- [47] C.-M. Chen, S. P. Kim, and J.-R. Sun, in *15th Marcel Grossmann Meeting on Recent Developments in Theoretical and Experimental General Relativity, Astrophysics, and Relativistic Field Theories* (2019) arXiv:1903.08881 [hep-th].
- [48] G. Veneziano, EPL **2**, 199 (1986).
- [49] P. Chen and R. J. Adler, Nucl. Phys. B Proc. Suppl. **124**, 103 (2003), arXiv:gr-qc/0205106.
- [50] K. Jusufi, Regular black holes in three dimensions and the zero point length (2022), arXiv:2209.04433 [gr-qc].
- [51] M. Takesaki, *Theory of Operator Algebras I* (Springer, 1979).
- [52] O. Bratteli and D. W. Robinson, *Operator Algebras and Quantum Statistical Mechanics 1* (Springer, 1987).
- [53] E. Witten, Rev. Mod. Phys. **90**, 045003 (2018), arXiv:1803.04993 [hep-th].
- [54] J. Kudler-Flam, S. Leutheusser, and G. Satishchandran, Phys. Rev. D **111**, 025013 (2025), arXiv:2309.15897 [hep-th].
- [55] R. M. Wald, *Quantum field theory in curved spacetime and black hole thermodynamics* (University of Chicago press, 1994).
- [56] J. Dimock, Communications in Mathematical Physics **77**, 219 (1980).
- [57] K. Prabhu, G. Satishchandran, and R. M. Wald, Phys. Rev. D **106**, 066005 (2022), arXiv:2203.14334 [hep-th].
- [58] T. Faulkner, R. G. Leigh, O. Parrikar, and H. Wang, JHEP **09**, 038, arXiv:1605.08072 [hep-th].
- [59] D. L. Jafferis, A. Lewkowycz, J. Maldacena, and S. J. Suh, Journal of High Energy Physics **2016**, 1 (2016).
- [60] A. Raychaudhuri, Physical Review **98**, 1123 (1955).